Interactive 3D Visualization of a Single-View X-Ray Image

Matthias Wieczorek[1], André Aichert[1], Pascal Fallavollita[1], Oliver Kutter[2], Ahmad Ahmadi[1], Lejing Wang[1], and Nassir Navab[1]

[1] Chair for Computer Aided Medical Procedures (CAMP), Technische Universität München, Munich, Germany
[2] Siemens Corporate Research, Princeton, NJ, USA
wieczore@cs.tum.edu

Abstract. In this paper, we present an interactive X-Ray perceptual visualization technique (IXPV) to improve 3D perception in standard single-view X-Ray images. Based on *a priori* knowledge from CT data, we re-introduce lost depth information into the original single-view X-Ray image without jeopardizing information of the original X-Ray. We propose a novel approach that is suitable for correct fusion of intra-operative X-Ray and ultrasound, co-visualization of X-Ray and surgical tools, and for improving the 3D perception of standard radiographs. Phantom and animal cadaver datasets were used during experimentation to demonstrate the impact of our technique. Results from a questionnaire completed by 11 clinicians and computer scientists demonstrate the added value of introduced depth cues directly in an X-Ray image. In conclusion, we propose IXPV as a futuristic alternative to the standard radiographic image found in today's clinical setting.

1 Introduction

For almost all medical imaging modalities, current state of the art visualization systems provide advanced techniques for real-time *direct volume rendering* (DVR), which is used for diagnosis, planning, and intra-operative procedures [5]. Fused visualization of co-registered, multi-modal image data of the patient and traditional surface based rendering, e.g. tracked instruments, implant models, or segmentation has become common practice [4,11]. Furthermore, depth perception has been an important field of research in computer graphics. Especially for DVR many methods for enhancing depth cues have been proposed [1,2,4,11,12]. For translucent volumes (such as X-Ray) an existing method uses stereoscopy [8]. However, little interest has been taken in transferring the advances in DVR to introduce additional depth cues to single X-Ray images. The intensities displayed in an X-Ray image go back to the attenuation of a complete ray traversal through the body and do not correspond to a specific depth along the ray. This also makes fusion of rendered objects with X-Ray images more difficult.

G. Fichtinger, A. Martel, and T. Peters (Eds.): MICCAI 2011, Part I, LNCS 6891, pp. 73–80, 2011.

Current state of the art methods use either 2D blending [10] with a user defined blending factor (i.e. common 2D/3D registration algorithms) or depth-of-field based 2D blending, which defines the blending factor per pixel according to the depth of the geometry. Both methods have the same major drawback: they do not account for the physics of X-Ray. Thus, the resulting fused image will provide inaccurate and frequently misleading depth cues (see Fig. 3 (center), (right)) making it hard for the user to correctly estimate distances and positions of objects from the fused view. The objective of our work is to propose a novel visualization technique for improving visual perception in general and depth perception in particular in medical X-Ray images. Our idea termed *Interactive X-Ray Perceptual Visualization* (IXPV) allows the user to interactively manipulate a single-view X-Ray image by varying depth. This is achieved by retrieving *a priori* knowledge of absorptive properties from CT data (pre-operative or atlas). Through phantom and animal cadaver experimentation and user study, we show that the IXPV technique introduces depth cues in X-Ray image visualization to disambiguate the ordering of internal structures or instruments used in everyday diagnostic and intraoperative scenarios. Possible applications for this method range from X-Ray based medical Augmented Reality to fusion of X-Ray and DVR renderings of volumetric data, such as PET scans.

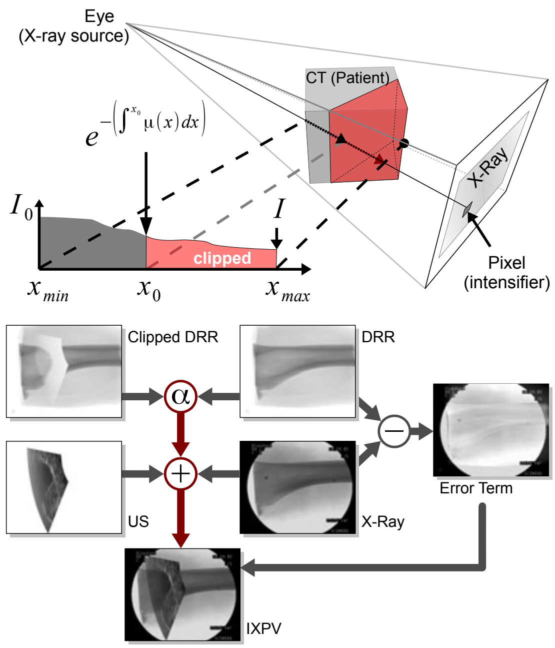

Fig. 1. (top) Classical analogy of DRR creation and X-Ray, after the CT (cube) has been registered. The figure also shows the effect of clipping the red portion of the CT on the attenuation function. (bottom) The major steps in IXPV rendering. α represents the coefficient used to modulate X-Ray and US (red arrows and +). Also shown is the error term from Section 2.7.

2 Methods

The proposed method aims at transferring information from co-registered CT data directly into X-Ray images. There exist several algorithms facing the problem of CT/X-Ray co-registration. There are marker, landmark and intensity based [9,10] methods. One could even think of using an Atlas CT i.e utilizing methods as proposed in [3] or [7]. In our method, we assume that we have a registration between CT and X-Ray using any of the aforementioned methods. All derivations below shield one goal: calculation of the X-Ray intensities at any depth along a certain ray by modulating the X-Ray image and not simply copying pixel values from *Digitally Reconstructed Radiograph* (DRR).

2.1 Beer-Lambert Law and X-Ray Intensities at Specific Depth

For an emitted dose of X-Ray radiation I_0, the Beer-Lambert law for linear X-Ray attenuation describes the intensity I at the end of a ray:

$$I = I_0 * e^{-\int \mu(x)dx} \tag{1}$$

where $\mu : [0,1]^3 \rightarrow [0,1]$ is the X-Ray absorption function. A CT is essentially a discrete volume of absorption values measured in Hounsfield Units. Thus the absorption is given by $\mu_{\text{CT}} = g \circ f$, where $f : [0,1]^3 \rightarrow [0,1]$ is a function defined by the CT and $g : [0,1] \rightarrow [0,1]$ is the *transfer function* (TF) mapping the values from CT to the correct absorption value [9].

For a moment, assume X-Rays were cut off at some specific depth. We are interested in the X-Ray intensity up to a specific point x_0 along this ray, as if the intensifier were placed there (compare Fig. 1 (top)). As the absorption function is monotonic decreasing this is valid and with Eq. 1 we derive:

$$I = I_0 * e^{-(\int^{x_0} \mu(x)dx + \int_{x_0} \mu(x)dx} = I_0 * e^{-\int^{x_0} \mu(x)dx} * e^{-\int_{x_0} \mu(x)dx} \tag{2}$$

Since luminance values are $\in [0,1]$, choose $I_0 = 1$, for maximal radiation:

$$e^{-\int^{x_0} \mu(x)dx} = I/e^{-\int_{x_0} \mu(x)dx} \quad \text{and} \quad e^{-\int_{x_0} \mu(x)dx} = I/e^{-\int^{x_0} \mu(x)dx} \tag{3}$$

2.2 Transfer of Information to X-Ray

Assuming exact registration (for discussion on error see section 2.7), this leads to an approximative absorption function $\mu_{\text{CT}} \approx \mu \quad \forall x \in [0,1]^3$. Using Eq. 3:

$$e^{-\int^{x_0} \mu(x)dx} = I_{\text{X-Ray}}/e^{-\int_{x_0} \mu(x)dx} \approx I_{\text{X-Ray}}/(\frac{I_{\text{CT}}}{e^{-\int^{x_0} \mu_{\text{CT}}(x)dx}}) \tag{4}$$

$$\Rightarrow e^{-\int^{x_0} \mu(x)dx} \approx \underbrace{I_{\text{X-Ray}}}_{\text{X-Ray value}} * \underbrace{\frac{e^{-\int^{x_0} \mu_{\text{CT}}(x)dx}}{e^{-\int \mu_{\text{CT}}(x)dx}}}_{\text{blending factor}} \tag{5}$$

We derive a blending factor for the original X-Ray image, which we use to modulate intensity information of geometry or another modality for a specific depth. The blending factor is defined as the quotient of two DRR-passes. The full DRR (denominator) I_{CT} has to be computed once for a given X-Ray image and the clipped DRR (numerator) has to be updated if x_0 (i.e. the object boundary) changes and only for pixels where an object is present.

2.3 Interactive X-Ray Perceptual Visualization (IXPV)

Given the registration between CT or atlas CT and the X-Ray images and the method proposed in 2.2, we can interactively manipulate the depth information across the co-registered X-Ray image. In fact, in general terms many interactive manipulations done on particular 3D views of CT images could be duplicated using only modulated X-Ray values. The image could be a static X-Ray view or a running fluoroscopic sequence.

2.4 Clipping X-Ray

The estimation of variation in the X-Ray pixels are given in Eq. 5. We could thereby manipulate X-Ray for better 3D perception, using general CT or Atlas CT data while only using the X-Ray pixel values. In our experiments we use a clipping plane to interactively examine the X-Ray image (see Fig. 2).

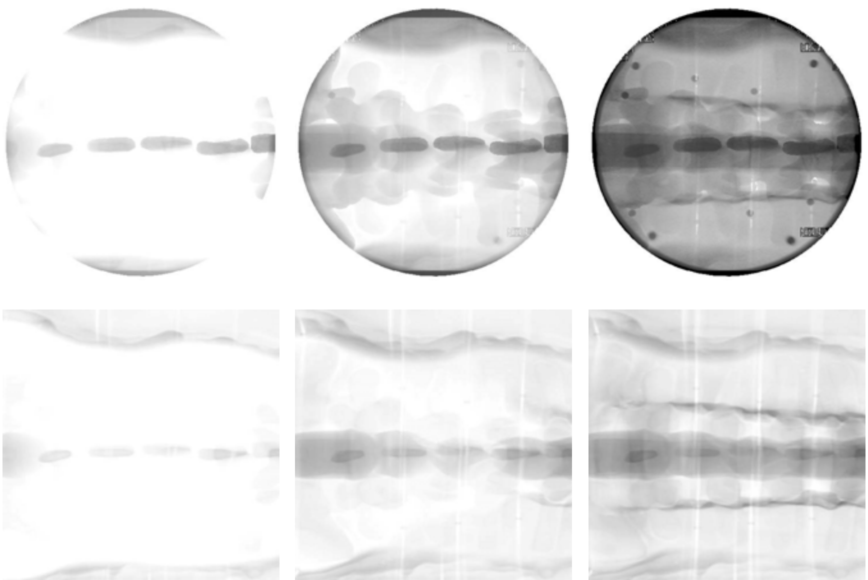

Fig. 2. Figures on top (round) show the result of IXPV of a clipping plane moving away from the viewer parallel to the image plane. Bottom figures (square) show corresponding clipped DRRs.

2.5 Fusion of Tools and X-Ray

Given a CAD model of a surgical tool and the possibility to track this tool, the virtual instrument can be directly fused with a given X-Ray image using IXPV and cutting the X-ray at the position where the virtual model of the tool is located. The results of our method are shown in Fig. 3 (left).

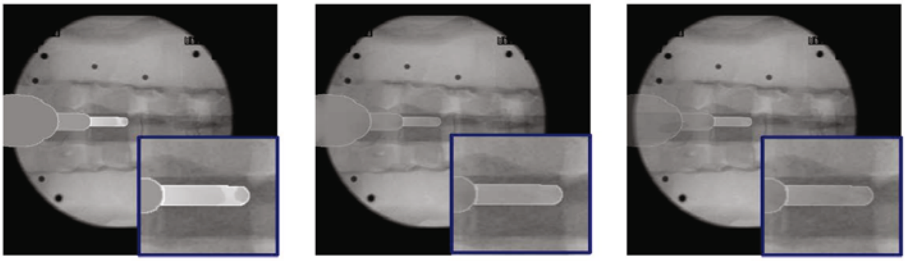

Fig. 3. A CAD model of a surgical drill fused with a single-view X-Ray image of a spine phantom. Compare IXPV (left) depth-of-field (center) and 2D blending (right).

2.6 Visualization of Co-registered X-Ray and Dynamic US

The visualization of fused X-Ray and ultrasound can take advantage of the depth cues given by IXPV. In this regard, the method implicitly takes occlusion related effects of the ultrasound plane and the X-Ray into account. For our experiments, a cow leg cadaver was positioned at the center of a transparent box with 6 reflective markers affixed to it that are visible in both CT and tracked NDI technology. Fusion between CT and ultrasound was realized using intensity based registration [6]. Having an accurate initial pose to an AP view of X-Ray, we fuse a B-mode ultrasound plane directly with X-Ray. Fig. 4 shows the effects of this fusion in comparison to 2D blending.

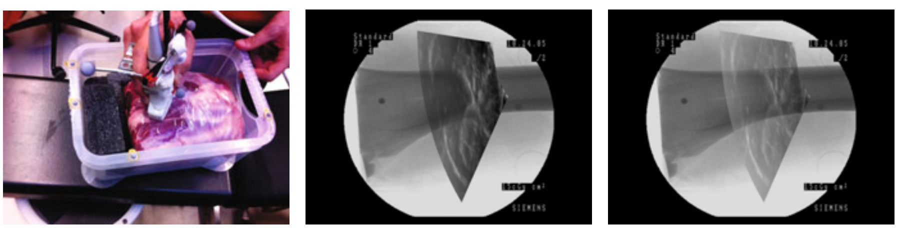

Fig. 4. Animal cadaver cow leg (left) visual assessment. (center) When applying the IXPV technique the tibia is displayed correctly in front of the ultrasound plane. Fusion using 2D blending of ultrasound and X-Ray (right) produces misleading depth cues.

2.7 Radiometric Error

Even if geometric 2D/3D registration of X-Ray and CT or Atlas could be done precisely thanks to recent advances in registration techniques, the estimation of the X-Ray intensity images is extremely difficult. This is due to 2D/3D registration optimizing a linear projection matrix while radiometric property estimation is a highly non linear procedure. The absorption value obtained from Eq. 5 is $\in [I_{\mathrm{XRay}}, \frac{I_{\mathrm{XRay}}}{I_{\mathrm{CT}}}]$. As for the difficulties of radiometric estimation: $\frac{I_{\mathrm{XRay}}}{I_{\mathrm{CT}}} \neq 1$.

To achieve reasonable visualization, (i.e. when integrating tracked instruments into X-ray using our method), we would like to have the object (i.e. instrument) fully visible in front of the anatomy. When moving behind anatomy only the X-Ray intensities should prevail. This intuition in mind we quantify the error in Eq. 5 as:

$$e^{-\int^{x_0}\mu(x)dx} - \frac{I_{\text{XRay}}}{I_{\text{CT}}} * e^{-\int^{x_0}\mu_{\text{CT}}(x)dx} \tag{6}$$

Note that for $x_0 = 0$ (in front of the volume) this leads to: $1 - \frac{I_{\text{XRay}}}{I_{\text{CT}}}$. For $x_0 = 1$ this corresponds to no error. Thus we decided to add

$$\frac{x_{\max} - x}{x_{\max} - x_{\min}} * (1 - \frac{I_{\text{XRay}}}{I_{\text{CT}}}) \tag{7}$$

to Eq. 5 in order to get the described visual effects, where $x_{\max}$ and $x_{\min}$ would define the limits of our volume of interest along the ray.

2.8 Error from Registration in Depth

A common issue for 2D/3D registration algorithms is that they are least reliable in depth. Let δx be this error in depth. For IXPV the absorption function approximation (Eq. 5) becomes $\mu_{\text{CT}}(x + \delta x) \approx \mu(x)$. Thus the error results in an offset within the intensity approximation and the error is given by:

$$e^{-\int^{x_0}\mu_{\text{CT}}(x+\delta x)dx} - \frac{I_{\text{XRay}}}{I_{\text{CT}}} * e^{-\int^{x_0}\mu_{\text{CT}}(x)dx} \approx e^{-\int^{x_0}\mu_{\text{CT}}(x+\delta x)dx} - e^{-\int^{x_0}\mu_{\text{CT}}(x)dx} \tag{8}$$

3 Results

The impact of our IXPV technique was validated through a series of phantom and cadaver experiments. For comparison, we also implemented 2D blending and depth-of-field techniques (see Fig. 3). The phantom study used co-registered CT and X-Ray of a spine phantom. A questionnaire was devised which is divided into two sections: depth perception in X-Ray and depth perception of clipping planes to evaluate the effect of interactivity. In total, eleven participants took part in the study (five experienced clinicians in the orthopedic and trauma surgery department and six senior researchers having a strong background in medical imaging). For section one (depth perception), we presented one top view composing a virtual model of a drill and the X-Ray, using either: (a) 2D blending (2D), (b) depth-of-field blending (dof) or (c) IXPV picture (compare Fig. 3). Participants were asked to choose correctly one out of three lateral views for the given top view. In a series of 27 questions, we randomized drill position depths (2, 5, or 10 millimeters), as well as the techniques.

3.1 User-Study

Participants received the following instructions for section two (X-Ray clipping): to choose correctly one of three lateral views given a static AP view and given videos of a clipping plane repeatedly moving through the object. In a series of 8 questions, we randomized between static image and video sequences. We accumulated statistical results of the questionnaire based on the total number of correct answers from all participants. Lastly, we asked only the surgeons to evaluate in a five-point Likert scale (i.e. 1 strongly disagree, 5 strongly agree), if IXPV was easier, more intuitive and more helpful for depth perception in X-Ray. A Wilcoxon rank sum test was used to calculate the p-values. *Depth perception:* The results for the three modes are presented in Fig. 5 (right). The p-value for IXPV vs. 2D blending turned out to be 0.0449 (significant). For IXPV vs. depth-of-field it is 0.0758 (not significant). *X-Ray interactive clipping:* The results are shown Fig. 5 (right). The p-value is 0.0119 (significant). *Likert scale:* The five surgeons responded positively to the IXPV method as suggested by a score of 3.7 ± 0.9.

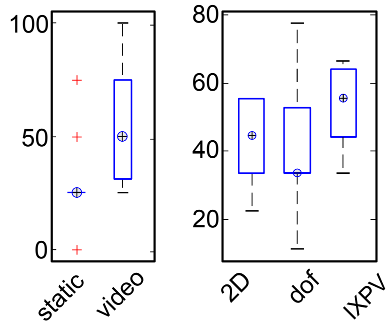

Fig. 5. Boxplots of the results

4 Discussion and Conclusion

This paper presents a novel technique of interactive X-Ray perceptual visualization (IXPV) which takes the physics of X-Ray into account to improve 3D perception within a single X-Ray image and allows fusion with tracked surgical tools or intraoperative ultrasound. Given an X-Ray image and a registered CT, our method relies on DVR algorithms to gain a modulation of original X-Ray intensities, to approximate those of a specific depth within the volume. Modern DVR algorithms and optimizations described in section 2.2 enable real-time visualization of IXPV even on low end graphics hardware. We evaluated our method using a survey which was designed to test two major hypotheses. Firstly, our method is superior to 2D blending. Although we were not able to reject the null hypothesis for IXPV vs. depth-of-fied blending, the results suggest, that IXPV provides more consistent depth cues than DOF. Secondly, our method enhances depth perception of 2D X-Ray images by allowing interactive examination with a clipping plane. Results suggest that IXPV should be further investigated and developed as a futuristic complimentary imaging tool to traditional radiographic images found in clinics. Future work includes the use anatomic models and/or of statistical atlas CT instead of patient specific data as well as fusion of IXPV with volumetric data, such as PET scans.

References

1. Boucheny, C., Bonneau, G.P., Droulez, J., Thibault, G., Ploix, S.: A perceptive evaluation of volume rendering techniques. In: Proceedings of the 4th Symposium on Applied Perception in Graphics and Visualization, APGV 2007, pp. 83–90. ACM, New York (2007)
2. Bruckner, S., Gröller, E.: Enhancing depth-perception with flexible volumetric halos. IEEE Transactions on Visualization and Computer Graphics 13, 1344–1351 (2007)
3. Chintalapani, G., Murphy, R., Armiger, R.S., Lepisto, J., Otake, Y., Sugano, N., Taylor, R.H., Armand, M.: Statistical atlas based extrapolation of ct data. In: Proceedings of SPIE, vol. 7625, p. 762539 (February 2010)
4. Díaz, J., Vazquez, P.: Depth-enhanced maximum intensity projection. In: IEEE/EG International Symposium on Volume Graphics, vol. 8, pp. 1–8 (2010)
5. Ebert, D., Rheingans, P.: Volume illustration: non-photorealistic rendering of volume models. In: Proceedings of the Conference on Visualization, VIS 2000, pp. 195–202. IEEE Computer Society Press, Los Alamitos (2000)
6. Fallavollita, P., Aghaloo, Z.K., Burdette, E.C., Song, D.Y., Abolmaesumi, P., Fichtinger, G.: Registration between ultrasound and fluoroscopy or ct in prostate brachytherapy. Medical Physics 37(6), 2749–2760 (2010)
7. Gong, R.H., Stewart, J., Abolmaesumi, P.: Reduction of multi-fragment fractures of the distal radius using atlas-based 2d/3d registration. In: Proceedings of SPIE. Medical Imaging 2010: Visualization, Image-Guided Procedures, and Modeling, Orlando, Florida, USA, vol. 7261, p. 726137 (February 2009)
8. Kersten, M., Stewart, J., Troje, N., Ellis, R.: Enhancing depth perception in translucent volumes. IEEE Transactions on Visualization and Computer Graphics 12, 1117–1124 (2006)
9. Khamene, A., Bloch, P., Wein, W., Svatos, M., Sauer, F.: Automatic registration of portal images and volumetric CT for patient positioning in radiation therapy. Medical Image Analysis 10(1), 96–112 (2006)
10. Markelj, P., Tomazevic, D., Likar, B., Pernus, F.: A review of 3d/2d registration methods for image-guided interventions. Medical Image Analysis (2010)
11. Svakhine, N.A., Ebert, D.S.: Interactive volume illustration and feature halos. In: Proceedings of the 11th Pacific Conference on Computer Graphics and Applications, PG 2003, p. 347. IEEE Computer Society, Washington, DC (2003)
12. Svakhine, N.A., Ebert, D.S., Andrews, W.M.: Illustration-inspired depth enhanced volumetric medical visualization. IEEE Transactions on Visualization and Computer Graphics 15, 77–86 (2009)